Incoherent scatter radar plasma density measurements at Jicamarca using a transverse-mode differential-phase method

Erhan Kudeki,[1] Ronald F. Woodman,[2] and Zhaomei Feng[1]

Received 16 May 2002; revised 2 September 2002; accepted 26 December 2002; published 14 March 2003.

[1] The 50 MHz Jicamarca incoherent scatter radar can be used to make very high precision F-region plasma drift measurements with less than a m/s uncertainty and 5 min/15 km time/height resolutions. In such measurements the transmitting antenna beam is pointed perpendicular to the geomagnetic field $\vec{B}$ [e.g., *Kudeki et al.*, 1999] and backscattered fields consist of magneto-ionic O- and X-components with unequal phase retardations. Detecting the fields with an orthogonal pair of linear-polarized antennas and fitting the average power and differential-phase of the antenna outputs to an appropriate data model we have succeeded in making F-region electron density measurements with data collected during Jicamarca drifts experiments. This procedure provides Jicamarca with a new capability for simultaneous drifts and density measurements at F-region heights. *INDEX TERMS:* 6969 Radio Science: Remote sensing; 2415 Ionosphere: Equatorial ionosphere; 6934 Ionospheric propagation (2487); 6994 Instruments and techniques. **Citation:** Kudeki, E., R. F. Woodman, and Z. Feng, Incoherent scatter radar plasma density measurements at Jicamarca using a transverse-mode differential-phase method, *Geophys. Res. Lett.*, *30*(5), 1255, doi:10.1029/2002GL015496, 2003.

1. Introduction

[2] A new incoherent scatter radar technique is being developed at Jicamarca for making F-region electron density measurements with antenna beams pointed perpendicular to the geomagnetic field. The project aims to provide density results to accompany the high-precision F-region drifts data collected using the same beam orientations [e.g., *Kudeki et al.*, 1999]. The purpose of this paper is to describe the new technique and present preliminary results obtained so far.

[3] The relative orientations of the geomagnetic field $\vec{B}$ and the radar beam above Jicamarca influence both the Doppler frequency spectrum and propagation phase delay of magneto-ionic subcomponents of backscattered radar fields. When the beam is perpendicular to $\vec{B}$ the fields are transverse propagating linear-polarized magneto-ionic modes [e.g., *Ratcliffe*, 1962] and have a relatively narrow frequency spectrum [e.g., *Kudeki et al.*, 1999]. But when the radar beam deviates from the transverse direction by as little as a few degrees the frequency spectrum is severely broadened and propagation is in terms of nearly circular polarized quasi-longitudinal modes. At the 50 MHz operation frequency of the Jicamarca radar, the critical angle which separates the quasi-longitudinal and -transverse regimes of ionospheric propagation is only about 0.5° off the direction perpendicular to $\vec{B}$.

[4] Since high-precision drifts measurements favor radar return signals with the narrowest possible frequency spectra, Jicamarca drifts observations are conducted using the linear-polarized transverse radar beams rather than the circular-polarized quasi-longitudinal beams used in Faraday rotation density measurements [*Farley*, 1969]. To supplement the Jicamarca drifts data with F-region density estimates we now collect the transverse-beam signal returns using an orthogonal pair of linear-polarized antennas and fit the average power and phase difference of the antenna outputs to an appropriate data model described in section 2. The new procedure is partly an extension of the Faraday rotation method [*Farley*, 1969] into the magneto-ionic regime of nearly linear polarized quasi-transverse propagation modes and partly a procedure of *Valladares and Woodman* [2001] based on collecting all components of the backscattered radar signal power. It is also based on the principles of maximum-likelihood data inversion [e.g., *Menke*, 1989].

[5] Preliminary results obtained with the new density estimation technique will be presented and discussed in section 3. Since the new technique makes use of a single beam direction it avoids the reduced sensitivity problem of the earlier Jicamarca drifts and density experiments [e.g., *Woodman et al.*, 1972] conducted with multiple beams. Also, as discussed in section 3, the technique holds the promise to provide electron density estimates within equatorial spread-F layers and bubbles.

2. Data Acquisition and Inversion

2.1. Orthogonal Receiver Signals

[6] The antenna array at Jicamarca consists of two orthogonal sets of half-wave dipoles with south-east and north-east polarizations, respectively. In reception mode we call the baseband voltage of the sum and difference of the orthogonal array outputs (obtained by using a hybrid-combiner prior to coherent detection) $V_\circ$ and V_θ. The sum $V_\circ$ is a complex voltage that samples the zonal component of the backscattered electric field. The difference V_θ samples the meridional component.

[7] When Jicamarca antenna beams are steered to point perpendicular to the geomagnetic field $\vec{B}$, the radar output voltages V_θ and $V_\circ$ correspond to respective samples of linear-polarized ordinary- and extraordinary-mode radar returns parallel and perpendicular to $\vec{B}$. The differential phase (in radians) of V_θ and $V_\circ$ is then

$$\angle V_\theta V_\circ^* = -2k_o \int_0^z dz' \delta n(z') \approx -\frac{80.6\Omega^2}{cf^2\omega} \int_0^z dz' N(z'), \qquad (1)$$

[1]Department of Electrical and Computer Engineering, University of Illinois at Urbana-Champaign, Urbana, Illinois, USA.
[2]Instituto Geofisico del Peru, Lima, Peru.

0094-8276/03/2002GL015496$05.00

where $\delta n \equiv n_o - n_x$ is the difference in ordinary- and extraordinary-mode refractive indices n_o and n_x, $80.6 \approx \frac{e^2}{m_e \epsilon_o}$ in MKS units, Ω the electron gyro-frequency, $k_o \equiv \frac{\omega}{c}$, $\omega = 2\pi f$ the radar frequency, z the scattering height, and $N(z)$ the ionospheric electron density profile. Expression (1) differs from the differential-phase of the right- and left-circular modes used in Faraday rotation method [*Farley*, 1969] by only a multiplicative factor of $\frac{\Omega/\omega}{2\cos\theta_o} \approx 0.15$, where $\theta_o \approx 87°$ is the Jicamarca beam pointing angle in the Faraday mode away from $-\vec{B}$. Expression (1) therefore suggests the possibility of inferring the ionospheric density profile $N(z)$ from the differential phase of the orthogonal components of transverse-beam radar returns.

[8] However, since the Jicamarca beams have a finite angular width and because the magnetic field vector $\vec{B}$ varies with altitude, the scattered signals are not strictly linear polarized and propagate in mixture with elliptic polarized quasi-transverse O- and X-modes. As a consequence, the inversion process used to estimate $N(z)$ from the transverse beam radar data requires a more accurate differential-phase model than just (1). The inversion process described next also makes use of backscattered power data P_θ and $P_\circ$ measured in θ - and ϕ-channels, respectively.

2.2. Data Models and Data/Model Misfit

[9] Let P_θ and $P_\circ$ denote the measured average power in θ - and ϕ-channels of a transverse-beam incoherent scatter radar experiment outlined above. Ideally then, $\langle P_{\theta,\circ}\rangle = \langle|V_{\theta,\circ}|^2\rangle$ —where $\langle\cdot\rangle$ denotes expected value—but in practice $\langle P_\theta\rangle = \langle|V_\theta|^2\rangle + A_\theta$ and $\langle P_\circ\rangle = |g|^2\langle|V_\circ|^2\rangle + A_\circ$ because of additive noise power $A_{\theta,\circ}$ in reception channels and relative voltage gain g of ϕ-channel receiver over the θ-channel receiver. Thus,

$$P \equiv |g|^2 P_\theta + P_\circ = |g|^2\Big(\langle|V_\theta|^2\rangle + \langle|V_\circ|^2\rangle\Big) + |g|^2 A_\theta + A_\circ + \delta P, \tag{2}$$

where δP is a zero-mean random fluctuation in $|g|^2 P_\theta + P_\circ$ about its expected value $|g|^2\langle P_\theta\rangle + \langle P_\circ\rangle$.

[10] Likewise, let ψ denote the phase angle of the estimate of the complex cross-correlation of θ- and ϕ-channel signals. Although $\langle\psi\rangle = \angle\langle V_\theta V_\circ^*\rangle$ ideally, in practice

$$\psi = \angle\langle V_\theta V_\circ^*\rangle - \angle g + \delta\psi \tag{3}$$

because of the phase $\angle g$ of relative gain g as well as random fluctuations $\delta\psi$.

[11] Relations (2) and (3) apply at every data range gate z_m where the power and phase data will be labeled as $P_{\theta m}$, $P_{\circ m}$, ψ_m and the corresponding data models as $\langle|V_\theta|^2\rangle_m + \langle|V_\circ|^2\rangle_m$, $\angle\langle V_\theta V_\circ^*\rangle_m$. With sufficiently long integration times used to compute $P_{\theta,\circ m}$, ψ_m, the corresponding fluctuations

$$\delta P_m \equiv |g|^2(P_{\theta m} - A_\theta) + (P_{\circ m} - A_\circ) - |g|^2\Big(\langle|V_\theta|^2\rangle_m + \langle|V_\circ|^2\rangle_m\Big) \tag{4}$$

and

$$\delta\psi_m \equiv \psi_m + \angle g - \angle\langle V_\theta V_\circ^*\rangle_m \tag{5}$$

are known to be independent zero-mean Gaussian random variables with a joint pdf $\propto e^{-\chi^2}/2$, where

$$\chi^2 \equiv \sum_m \frac{\delta P_m^2}{\langle\delta P_m^2\rangle} + \sum_m \frac{\delta\psi_m^2}{\langle\delta\psi_m^2\rangle}. \tag{6}$$

Furthermore, since χ^2 depends on ionospheric electron densities via $\langle|V_\theta|^2\rangle_m + \langle|V_\circ|^2\rangle_m$ and $\angle\langle V_\theta V_\circ^*\rangle_m$ in (4) and (5), the distribution $\propto e^{-\chi^2}/2$ also represents the joint likelihood of electron densities at sampling heights conditioned by ionospheric data $P_{\theta,\circ m}$, ψ_m. As a consequence we can determine the maximum-likelihood estimates of the densities by minimizing (6) over its free parameters. This procedure can be viewed as finding the best fit of the backscatter radar data to data models $\langle|V_\theta|^2\rangle_m + \langle|V_\circ|^2\rangle_m$ and $\angle\langle V_\theta V_\circ^*\rangle_m$ described next.

2.2.1. Power Model

[12] For matched-filtered reception of the echoes of uncoded radar pulses of some length Δz,

$$\langle|V_\theta|^2\rangle_m + \langle|V_\circ|^2\rangle_m = \frac{K}{z_m^2}\frac{N_m}{1+\mu_m} \equiv \Pi_m, \tag{7}$$

where K is a system constant (that depends on transmitted power, antenna aperture, Ohmic losses, pulse length Δz, etc.), N_m denotes the average electron density between the heights $z_{m-1} = z_m - \Delta z$ and $z_{m+1} = z_m + \Delta z$, and μ_m is a variable of order unity that depends on the electron-ion temperature ratio T_e/T_i within the same height range. Model Π_m is a consequence of incoherent scatter radar cross-sections $\propto N(z)(1 + \mu(z))^{-1}$ [e.g., *Farley*, 1971] and the principle of energy conservation (ignoring the differential absorption of O- and X-modes which is negligible at 50 MHz), and is valid independent of the antenna polarizations used in pulse transmission. Although $\langle|V_\theta|^2\rangle_m$ and $\langle|V_\circ|^2\rangle_m$ will individually depend on the polarization of transmitted field and magneto-ionic propagation effects, the sum $\langle|V_\theta|^2\rangle_m + \langle|V_\circ|^2\rangle_m$ is independent of these factors since the orthogonal field samples V_θ and $V_\circ$ fully account for the scattered field and its entire power content whatever the polarization.

[13] Transmitter pulses used in Jicamarca drifts experiments have a 3-baud Barker code (++−) with a baud length of $\Delta z = 15$. Hence, to account for the power data obtained with Barker decoded signal samples we use in (4) the ideal data model

$$\langle|V_\theta|^2\rangle_m + \langle|V_\circ|^2\rangle_m = \Pi_{m-2} + 9\Pi_m + \Pi_{m+2} \tag{8}$$

which is a straightforward extension of (7).

2.2.2. Differential-Phase Model

[14] For transverse-propagating and linear-polarized radar returns (1) implies that

$$\angle\langle V_\theta V_\circ^*\rangle_m \approx -\frac{80.6}{cf^2\omega}\sum_{q=1}^{m}\Omega_q^2 N_q \Delta z \equiv \Psi_m, \tag{9}$$

where $\Omega_q \equiv \Omega(z_q)$, product $N_1\Delta z$ represents the total electron content of lower ionosphere below the lowest usable data range gate z_1, and, for $m > 1$, N_m is the average electron density between z_{m-1} and z_{m+1}. However, when the effect of elliptic-polarized radar returns propagating in slightly off-transverse directions is taken into account, a small correction term $\delta\Psi_m$ needs to be added to Ψ_m. Therefore, in (5) we use

$$\angle\langle V_\theta V_\circ^*\rangle_m = \Psi_m + \delta\Psi_m, \tag{10}$$

where the correction term $\delta\Psi_m$ is determined by considering the axial-ratio and differential-phase of backscattered returns propagating at an angle 0.38° away from the transverse

direction as explained in detail in a forthcoming paper by Z. Feng et al. (Transverse-beam incoherent scatter radar measurements of F-region plasma densities at Jicamarca, submitted to Radio Science, 2002, hereinafter referred to as Feng et al., submitted manuscript, 2002). The angle 0.38° used in $\delta\Psi_m$ calculations is the σ of a Gaussian curve that describes the shape of the two-way antenna gain pattern at Jicamarca after it has been integrated in zonal direction perpendicular to $\vec{B}$.

2.2.3. Data/Model Misfit

[15] From the viewpoint of least-squares data fitting (6) represents a global misfit between the data and data models described above. The computation and minimization of the misfit requires that its summation bounds over m be specified and data variances $\langle\delta P_m^2\rangle$, $\langle\delta\psi_m^2\rangle$ known. The summation bounds in turn depend on how accurately the variances can be specified.

[16] Let s_m denote the normalized cross-correlation of θ- and ϕ-channel outputs at range gate z_m and I the number of independent voltage products averaged to obtain the differential phase estimate ψ_m. Then, as shown in *Woodman and Hagfors* [1969], error $\delta\psi_m$ in ψ_m is a Gaussian random variable with a variance

$$\langle\delta\psi_m^2\rangle = \frac{1}{2I}\frac{1-|s_m|^2}{|s_m|^2} \tag{11}$$

provided that

$$|s_m| \gg \frac{1}{\sqrt{I}}. \tag{12}$$

Condition (12) can be satisfied only near and below the F-region peak because above the F-region peak $|s_m|$ decreases with increasing altitude as the signal-to-noise ratio (SNR) drops. For that reason the second sum in (6) is carried from $m = 1$ corresponding to the first data range gate $z_1 = 210$ km to some m above the F-region peak above which (12) is violated. The first sum in (6), on the other hand, is carried from $z_m = 300$ to 825 km using the variance formula

$$\langle\delta P_m^2\rangle = \frac{\langle P_m\rangle^2}{I} - \left(1-|s_m|^2\right)\frac{2|g|^2\langle P_{\theta m}\rangle\langle P_{\circ m}\rangle}{I}. \tag{13}$$

Power data for $z_m < 300$ km are excluded from (6) for a number of reasons including the dependence of (8) on unknowns μ_m.

[17] In computing $\langle\delta\psi_m^2\rangle$ and $\langle\delta P_m^2\rangle$ according to (11) and (13) we replace $|s_m|$ and $\langle P_m\rangle$, $\langle P_{\theta,\circ m}\rangle$ with their estimates obtained from the measured data. Also the value for I is determined from the time integration used to compute $P_{\theta,\circ m}$, ψ_m.

2.3. Data Inversion

[18] In section 2.2 we found out that given a set of radar data $P_{\theta,\circ m}$, ψ_m, misfit (6) is a function of ionospheric density samples N_m as well as parameters K, $|g|$ $\angle g$, $A_{\theta,\circ}$, and μ_m. We also know that $\mu_m = 1$ for $z_m \geq 450$ km (the altitude regime where $T_e/T_i \approx 1$ is expected) and we have fairly good estimates for the noise power $A_{\theta,\circ}$ obtained from the highest sampled range gates ($z_m = 840$ to 900 km) which are excluded from the χ^2 sum. Furthermore, we expect that $|g| \approx 1$ because the receiver gains were fairly well balanced during the experiment. Therefore, the best fit of the measured data to the models described in section 2.2 is obtained by minimizing

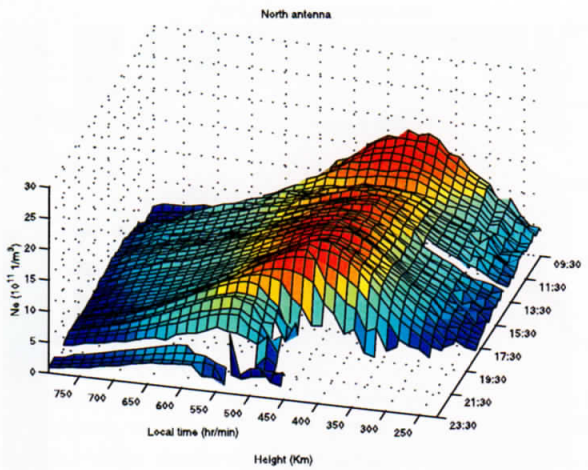

Figure 1. Surface plot of estimated plasma density N for January 9, 2000.

(6) over K, $|g|$, $\angle g$, $A_{\theta,\circ}$, μ_m (for $300 < z_m \leq 450$ km), and N_m subject to the constraints that (a) $A_{\theta,\circ}$ remain within a standard deviation of their independently determined estimates, and (b) $|g|$ remains close to 1. The constraints are enforced by adding to (6) terms which grow quadratically when $A_{\theta,\circ}$ and $|g|$ stray away from their expected values ("prior information" within a Bayesian framework). However, deviation of $|g|$ from 1 is not heavily penalized.

[19] The fit or data inversion procedure outlined above is applied to power and phase data $P_{\theta,\circ m}$, ψ_m obtained with 15 minutes of time integration. The inversion procedure is initiated with reasonable guesses for the unknowns which are subsequently adjusted iteratively using the Marquardt-Levenberg algorithm [e.g., *Press et al.*, 1988] until the modified χ^2 is minimized to a value on the order of the number of degrees of freedom of the problem. The convergence time per altitude profile is less than 10 s with a MATLAB code on a PC, i.e., a small fraction of an integration time, opening the possibility for real-time evaluations. System unknowns K, $|g|$, $\angle g$, as well as noise powers $A_{\theta,\circ}$ change very little from one profile inversion to the next.

[20] Before discussing the inversion examples shown in Figures 1 and 2 we need to describe a few more aspects of the inversion process. First, we note that it is not possible to lump the unknown $\angle g$ with the input N_1 of $\Psi_m + \delta\Psi_m$ model because of the nonlinear dependence of $\delta\Psi_m$ on N_1 described in Feng et al. (submitted manuscript, 2002). Thus the receiver phase $\angle g$ remains an independent free parameter of our inversion process. This does not cause a major difficulty as we find that the best fit values of $\angle g$ remain unchanged between profile inversions.

[21] Second, we note that the success of our density profile inversions depends crucially on having both power and phase data $P_{\theta,\circ m}$ and ψ_m at a sufficiently large number of range gates above 450 km where $\mu_m = 1$ is assumed. The mutual consistency of $P_{\theta,\circ m}$ and ψ_m variations over those range gates is effectively what determines the values of K, g, and $A_{\theta,\circ}$, and thus make density estimation possible in the lower and upper F-regions where either power or phase data are unreliable and/or not useful. Density estimates from upper F-region, for instance, only depend on power data combined with K, $|g|$, and $A_{\theta,\circ}$ coefficients since phase data are unreliable (and excluded from (6)) because of the

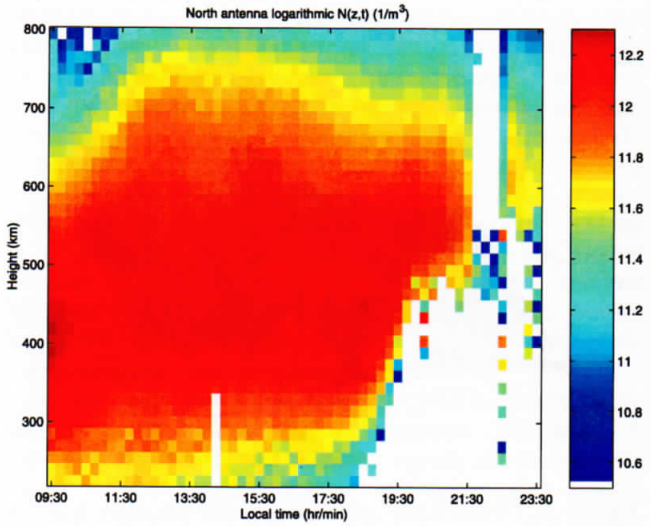

Figure 2. Map plot of $\log_{10}N$ estimates for January 9, 2000. Missing data in the evening sector are a consequence of receiver saturation due to spread-F echoes.

violation of (12). Conversely, for density estimates from lower F-region where μ_m is a free parameter (instead of unity) only the phase data matter. The reason is, whatever the power data, an unconstrained μ_m always adjusts itself during the inversion to cancel out δP_m exactly within (6). Therefore, power data $P_{\theta,\phi m}$ are superfluous for density estimation in the lower F-region unless μ_m is constrained based on some prior knowledge.

[22] It should be clear from above discussion that random fluctuations in lower F-region density estimates originating from phase errors $\delta\psi_m$ can be reduced or regularized [e.g., *Press et al.*, 1988] by preventing μ_m from fluctuating freely. One way of doing that which was used in the examples shown in Figures 1 and 2 is to penalize the deviations of μ_m from its neighbor μ_{m+1}. This is a reasonable constraint on μ_m since T_e/T_i is known to vary slowly with height. The constraint is enforced by adding a term $\alpha \sum_m (\mu_m - \mu_{m+1})^2$ to (6) before minimization. The sum in this new term is carried over $300 < z_m \leq 450$ km altitude region and the penalty coefficient α is taken (more or less) as the smallest value for which density noise in the same region is substantially reduced. Constrained as well as unconstrained (i.e., $\alpha = 0$) inversions typically yield μ_m values of 0.3 to 1.2 between 300 and 450 km altitudes. Also, as expected, constrained inversions result in smoother variations of μ_m and N_m with height. In the next section we will explain why $\mu_m < 1$ is reasonable when $T_e/T_i > 1$ at lower F-region heights.

3. Discussion

[23] Figures 1 and 2 display F-region plasma density estimates N_m, $m > 1$, as a function of sampling heights $z_m \equiv 210 + (m-1)$ 15 km obtained with the data inversion procedure described in section 2. The radar data used in the inversions were collected at the Jicamarca Radio Observatory on January 9, 2000, using the transverse beam geometry of the Jicamarca F-region drifts experiments and an interpulse period (IPP) of 6.6 ms. The transmitted radar pulses were coded using the ++− Barker code with a baud length of 15 km and the return signals were matched filtered in the baseband. Missing density data in Figures 1 and 2 in the evening sector are a consequence of receiver saturation due to equatorial spread-F echoes.

[24] The results presented Figures 1 and 2 should be regarded as preliminary as we are aware that the inversions can be improved by taking into account minor sources of systematic errors (e.g., I- and Q-channel misbalances, instrumental coupling between the θ- and ϕ-channels, small deviation of beam boresights from the transverse direction, etc.) as well as including in the procedure the Jicamarca ionosonde data. Also, with the wide dynamic range digital receivers being developed at Jicamarca it will be possible to detect the F-region returns without saturation problems even during spread-F conditions. Since phase noise will be substantially reduced during spread-F due to increased SNR we expect that it will be possible to make density measurements within equatorial spread-F layers and bubbles using the differential-phase data. Note that the height derivative of the differential-phase of spread-F echoes can be modeled in terms of linear polarized ordinary- and-extraordinary modes—just like (1)—since spread F irregularities are known to be highly field aligned and the variation of $\vec{B}$ within a single range gate is negligible.

[25] In our density estimation procedure we treat μ as a regularized unknown in the lower F-region since the latter depends on T_e/T_i which can deviate from 1 at those altitudes. The dependence is $\mu \approx T_e/T_i$ for longitudinal modes, but for transverse modes, $\mu \approx T_i/T_e$. Lower F region μ_m estimates which were found to be less than 1 in our inversions indicate that the backscattered fields were dominated by tranverse propagating contributions as expected.

[26] **Acknowledgments.** We appreciate inspired inputs and suggestions from Koki Chau and Farzad Kamalabadi and thank the staff and engineers of the Jicamarca Radio Observatory for their assistance with the observations. The Observatory is operated by Instituto Geofisico del Peru with support from the U. S. National Science Foundation. This work was supported by the Aeronomy Program, Division of Atmospheric Sciences of the NSF through grants ATM 99-11209 and ATM 02-15426.

References

Farley, D. T., Faraday rotation measurements using incoherent scatter, *Radio Sci.*, *4*, 143, 1969.

Farley, D. T., Radio wave scattering from the ionosphere, in *Methods of Experimental Physics*, vol. 9, part B, edited by R. H. Lovberg and H. R. Griem, Academic, San Diego, Calif., 1971.

Kudeki, E., et al., A new approach in incoherent scatter *F* region E × B drift measurements at Jicamarca, *J. Geophys. Res.*, *104*, 28,145, 1999.

Menke, W., *Geophysical Data Analysis: Discrete Inverse Theory*, Academic, San Diego, 1989.

Press, W. H., et al., *Numerical Recipes in C*, Cambridge Univ. Press, New York, 1988.

Ratcliffe, J. A., *The Magneto-ionic Theory*, Cambridge Univ. Press, New York, 1962.

Valladares, C. E., and R. F. Woodman, Comparison of Jicamarca densities and a numerical first-principle model of the low latitude ionosphere, paper presented at CEDAR meeting, Longmont, Colo., 2001.

Woodman, R. F., and T. Hagfors, Methods for the measurement of vertical ionospheric motions near the magnetic equator by incoherent scattering, *J. Geophys. Res.*, *74*, 1205, 1969.

Woodman, R. F., et al., Synthesis of Jicamarca data during the great storm of March 8, 1970, *Radio Sci.*, *7*, 739, 1972.

Z. Feng and E. Kudeki, Department of Electrical and Computer Engineering, University of Illinois, 1406 W. Green Street, Urbana, IL 61801, USA. (e-kudeki@uiuc.edu)

R. F. Woodman, Instituto Geofisico del Peru, Lima, Peru. (ronw@geo.igp.gob.pe)